

Dielectric Relaxation in Isotropic/Liquid Crystalline Block Copolymers: Effect of Nanoscale Confinement on the Local β and γ Dynamics

Sergei Zhukov,[†] Steffen Geppert,[‡] Bernd Stühn,^{*,†} Rosina Staneva,[†] and Wolfram Gronski[‡]

Technical Physics II/Polymer Physics, Ilmenau Technical University, PF 100565, 98684 Ilmenau, Germany, and Institute of Macromolecular Chemistry, Albert-Ludwigs-University, 79104 Freiburg, Germany

Received February 18, 2003

ABSTRACT: The effect of nanoscale confinement on the local polymer dynamics has been studied by means of dielectric spectroscopy in the frequency range from 10 mHz to 1 MHz. We have used microphase-separated PS/LC block copolymers (PS = polystyrene, LC = liquid crystalline). Depending on volume fraction, the LC blocks were confined to a layer with thickness of 21.3 and 11.2 nm (lamellae morphology) or were contained in domains of cylindrical or spherical form with diameter of 12.6 and 9.4 nm, respectively. At lower concentration of PS blocks, the LC copolymer form a continuous LC matrix with cylindrical inclusions of PS component. For all morphologies the LC block reveals two dielectric relaxations related to the local motion of mesogen (β process) and spacer (γ process). The relaxation time as well as the activation energy for the γ process was independent of spatial constraints even for the smallest characteristic length of 9.4 nm. The β relaxation, however, speeds up, and its activation energy decreases for confinement lengths less than 20 nm. The γ process has an essentially noncooperative nature, whereas the β process exhibits a positive apparent activation entropy, reflecting a partial cooperative feature. As a result, the β relaxation is affected by confinement just as the essentially cooperative dynamic glass transition (α relaxation) in polymers.

Introduction

Microphase-separated block copolymer systems offer the possibility to study the segmental dynamics of polymers in confined geometry. In such systems one or both blocks are confined to domains with well-defined dimensions typically ranging from a few to 100 nm.¹ The common types of domain forms are spheres, cylinders, and lamellae representing the cases of three- (3D), two- (2D), and one-dimensional (1D) confinement, respectively. Very few papers have so far been devoted to a study the effect of confinement on polymer dynamics in copolymers.^{2–4} It was shown that in the case of isotropic block copolymers with different morphologies not only the global (normal mode) but also segmental dynamics are affected by confinement.^{2,3} Recently, for polystyrene/liquid crystal (PS/LC) copolymers we have found that both cooperative modes (α and δ) observed in the LC block display decreased relaxation times if the domain size becomes less than 20 nm.⁴ In addition to this, we do not observe a strong change in the width of the α relaxation regime, reflecting the mobility of the main chain.

Recently, for thin polymer films, representing the case of 1D confinement, it was shown that the dynamic glass transition (α process) speeds up and its relaxation time distribution broadens as compared to the case of the bulk material.^{5–10} Moreover, in some work it was reported that the secondary β relaxation is also faster for film thickness less than 100 nm.^{8,10} The overall change in relaxation time for the β process was about 1 order of magnitude for *a*-PMMA films with thickness 1070 and 9.5 nm⁸ and slightly less in other work.¹⁰ In

later work the β relaxation was investigated for *i*-, *a*-, and *s*-PMMA thin films. Independent of tacticity, all polymers reveal a systematic speed-up in the local dynamics accompanied by a decrease of the relaxation strength. All these findings are rather unexpected because it is commonly assumed that the characteristic length for the secondary relaxation is short. It is assumed to be localized within several chemical bonds and hence is not expected to change under such a confinement. This point of view is confirmed by another study on *i*-PMMA thin films with thickness down to 18 nm, where the β process relaxation time as well as its relaxation strength was essentially independent of film thickness.⁹ To clarify this point, we have undertaken an investigation of PS/LC diblock copolymers, where the LC block is confined to microdomains with different size and shape. Such spatial constraints are formed as a consequence of the microphase separation between the isotropic PS and the mesomorphic LC blocks. The latter has the typical side-chain architecture, where the cyanobiphenyl mesogen fragment is connected to the main chain via a flexible methylene spacer.

It is known that the bulk (unconfined) side-chain LC polymers with cyanobiphenyl mesogen fragment and with four carbon methylene spacer reveal two local modes (called β and γ) related to the motion of mesogen and spacer, respectively.¹¹ Moreover, any chemical modification of chain structure (copolymer structure, H-bond, or/and network formation), which does not touch the side chain directly, does also not affect its local motion.¹¹ Thus, we expect to observe these local modes in the PS/LC block copolymers.

In the present work we have studied a series of nine PS/LC block copolymers and the LC homopolymer. Block volume fractions were varied systematically in the full range of compositions. The domain structure of these compounds was determined previously by means

[†] Ilmenau Technical University.

[‡] Albert-Ludwigs-University.

* To whom correspondence should be addressed.

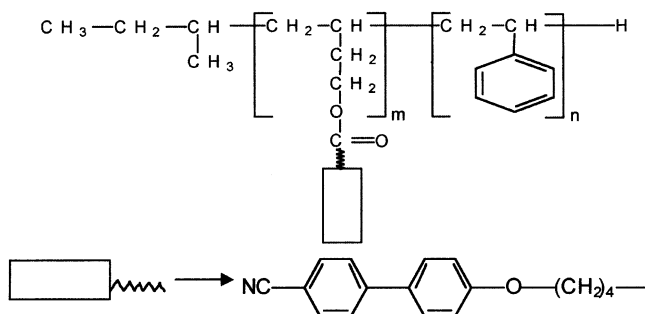


Figure 1. Chemical structure of copolymers under investigation.

Table 1. Mesophase Structure and Dimensions of the LC Block Obtained from the SAXS Data: Thickness of the LC Layer in the Lamellar Mesophase, δ_{LC} , and Radius of the Spherical or Cylindrical LC Domains in the Hexagonal and Cubic Mesophases, R_{LC}

polymer	mesophase	structure	δ_{LC} , R_{LC} [nm]
PSLC 7/93	hexagonal	PS cylinders in LC matrix	
PSLC 14/86	hexagonal	PS cylinders in LC matrix	
PSLC 19/81	hexagonal	PS cylinders in LC matrix	
PSLC 30/70	hexagonal ^a	PS cylinders in LC matrix	
PSLC 39/61	lamellar	PS and LC lamellae	21.3
PSLC 59/41	lamellar	PS and LC lamellae	11.2
PSLC 77/23	lamellar	PS and LC lamellae	11.2
PSLC 85/15	hexagonal	LC cylinders in PS matrix	6.3
PSLC 97/3	cubic	LC spheres in PS matrix	4.7

^a SAXS data are not well resolved.

of small-angle X-ray scattering.⁴ The LC homopolymer represents a continuous undisturbed matrix. Increase of the PS content results in a LC matrix with cylindrical inclusions of PS and to systems of alternating layers of PS and LC. At higher concentration of the PS blocks, the LC is contained in domains of cylindrical or spherical form. Summarizing the discussed features of systems under study, we may mention that the microphase-separated PS/LC copolymers represent an excellent case to study the confinement effect on local polymer motion.

2. Experimental Section

Synthesis and Characterization of the LC/PS Block Copolymers. The details of the synthesis of PS/LC copolymers and their characterization are described in ref 4. The LC block consists of cyanobiphenyl mesogens coupled to poly(1,2-butadiene) through valeric acid spacers (Figure 1).

The polymers are denoted as PSLC x/y , where x is the fraction of PS block in volume percent and y is the content of the LC block. The volume fraction of both blocks is varied and covers the full range of composition. All PS/LC diblock copolymers have a narrow molecular weight distribution with polydispersity index less than 0.1. DSC and polarized microscopy data reveal that the mesomorphic behavior of LC blocks is only slightly influenced by the copolymer composition and is basically characterized by the sequence $g/\sim 35^\circ\text{C}/n/\sim 120^\circ\text{C}/i$. As a result of the strong incompatibility between the PS block and the LC block, the polymers were found to be microphase-separated in the full temperature regime from 25 up to 170 °C. Table 1 summarizes the results obtained for the domain structure on the basis of the SAXS patterns. In all cases only one type of mesophase structure was obtained independent of the temperature.

Dielectric Spectroscopy (DS). Dielectric experiments in the frequency range from 10^{-2} to 10^6 Hz were carried out by measuring the complex impedance. We used a Solartron-Schlumberger frequency response analyzer SI 1260 equipped

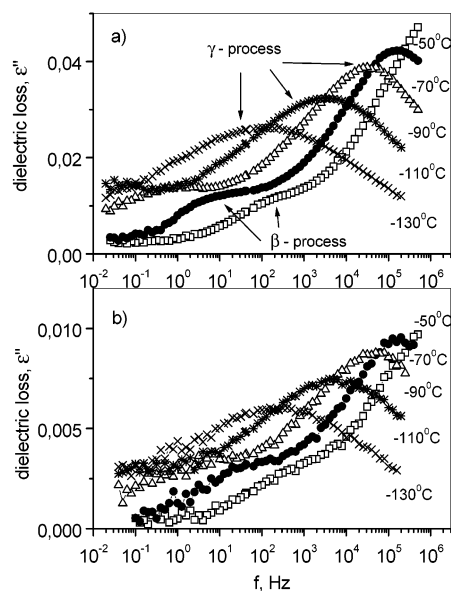


Figure 2. Dielectric spectra for PSLC 14/86 (a) and PSLC 77/23 (b) at different temperatures as indicated. The errors are smaller than the size of the symbols.

with a Chelsea dielectric interface. The sample capacitor consisted of two gold-coated stainless steel electrodes. It was filled with the polymer at 150 °C. The sample thickness was 0.05–0.1 mm. The sample temperature in the range –150 to 20 °C was controlled in a nitrogen gas jet (Quattro, Novocontrol GmbH) with a stability better than 0.05 °C. Dielectric data were collected at fixed temperature in heating and cooling runs with temperature steps of 5–10 deg, allowing for sample equilibration after each temperature change.

3. Experimental Results and Discussion

As an example, Figure 2 shows the dielectric spectra for the two copolymers with large (PSLC 14/86) and small (PSLC 77/23) LC volume fraction. As expected, the two relaxation processes denoted as β and γ are observed in the glassy state of these compounds. The other PS/LC copolymers studied also reveal these relaxation in this temperature–frequency window. The intensities of the β and γ processes are proportional to LC block content. Only for the PSLC 97/3 with the lowest LC content was it impossible to resolve the β transition due to its very low intensity. Since the PS block does not have any relaxation of dipole polarization at low temperatures, both processes are related to the LC block. As was already mentioned in the Introduction, many bulk side-chain LC polymers with a cyanobiphenyl mesogen fragment and methylene spacer reveal these relaxations.^{11,12}

To describe quantitatively the experimental spectra, the isothermal data of the dielectric losses ϵ'' were fitted to a superposition of two Havriliak–Negami (HN) functions:¹³

$$\epsilon''(\omega) = \sum_{k=1}^2 \text{Im} \left(\frac{\Delta\epsilon_k}{(1 + (i\omega\tau_k)^{\alpha_k})^{\gamma_k}} \right) \quad (1)$$

where ω is angular frequency ($= 2\pi f$), $\Delta\epsilon_k$ is the relaxation strength, and τ_k is the relaxation time of the k th process. The shape parameters α_k and γ_k describe the symmetric and asymmetric broadening of the relaxation peak, respectively. In the case of $\alpha = \gamma = 1$ the HN function reduces to that of a Debye relaxation process. Special cases are the symmetric Cole–Cole

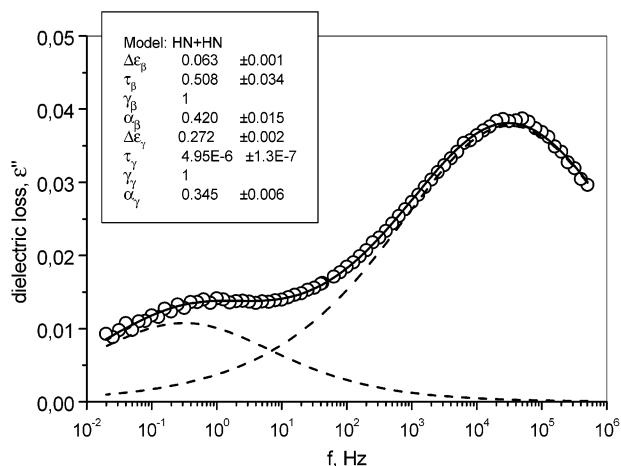


Figure 3. Example of the fitting results for the polymer PSLC 14/86 at -90.0°C . The solid line is the sum of the two dashed curves.

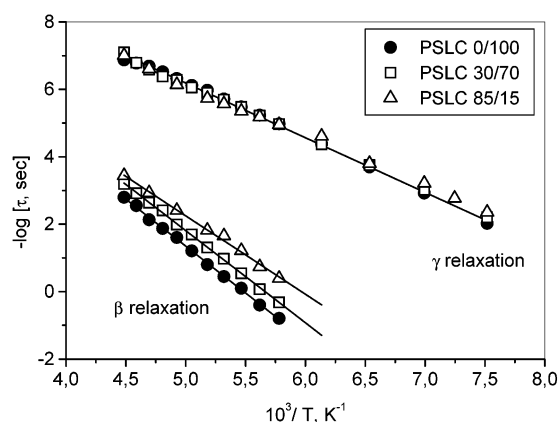


Figure 4. Activation diagram for the local relaxation processes in the copolymers investigated. The errors are smaller than the size of the symbols. The solid lines are the fit of eq 2 to the data.

function ($\alpha < 1$, $\gamma = 1$) or the asymmetric Cole–Davidson function ($\alpha = 1$, $\gamma < 1$).

Equation 1 is fitted to the experimental data using a nonlinear least-squares algorithm. It was shown previously that the local modes of the side-chain LC polymers are well described by the symmetric distribution of the relaxation times.¹⁴ So, we fix the shape parameter γ to be equal 1. After that the fit routine provides stable results for the relaxation times of β and γ processes for all copolymer studied. The accuracy in the determination of HN parameters was generally better than 10%. Figure 3 shows an example of the fitting results for the PSLC 14/86 at -90°C . It is seen that both relaxations are nicely separated using this procedure.

On the basis of the HN fit results, the activation diagram can be constructed. Figure 4 displays the activation diagram for both relaxation processes for selected copolymers and for the LC homopolymer. Both processes display a linear temperature dependence of the relaxation time in Arrhenius coordinates and hence can be described by an Arrhenius equation

$$\tau = \tau_0 \exp(E_a/kT) \quad (2)$$

where τ_0 is the preexponential factor and E_a is the activation energy. The activation energies determined from the slope of these curves are $E_{a\beta} \sim 53$ kJ/mol for the β process and $E_{a\gamma} \sim 30$ kJ/mol for the γ process. The

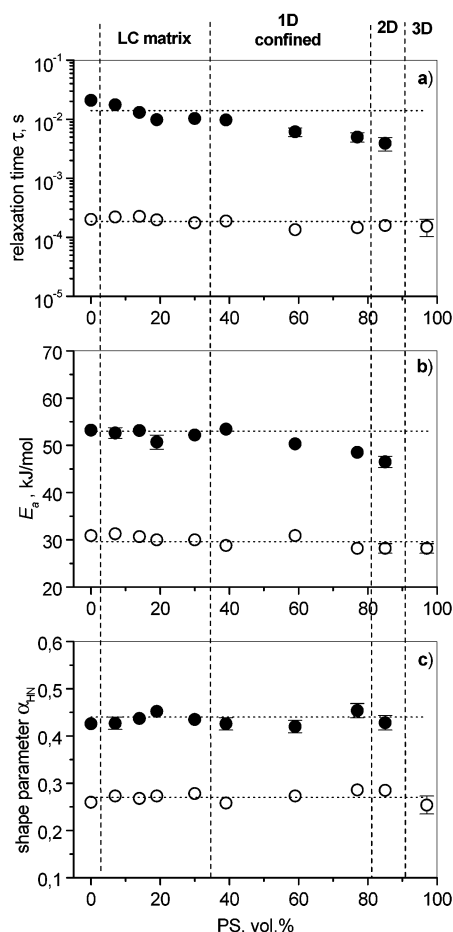


Figure 5. Relaxation time τ (a), activation energy E_a (b), and shape parameter α_{HN} (c) for the β (●) and γ (○) processes of LC block as a function of PS volume fraction. The relaxation time and shape parameter are given at -70°C for the β process and at -120°C for the γ process. The vertical dashed lines separate approximately the different mesophase structures. Here and below error bars are drawn wherever they exceed size of the symbols.

determined parameters for the β and the γ transitions have typical values of secondary or subglass relaxations. They reflect the reorientation of relatively small portions of the macromolecule.¹⁵

We now turn to the effect of variable domain form and size on local motion. Figure 5 shows the variation of the relaxation time τ , activation energy E_a , and shape parameter α_{HN} for different morphologies, i.e., for various spatial constraints. The LC block is continuously passing from the unconfined state (LC homopolymer and LC matrix) to the 1D (lamellae), 2D (cylinders), and 3D (sphere) spatial constraints on moving from the left to the right. Let us consider the γ relaxation first.

γ Relaxation. As is known from the literature, the γ process reflects the local spacer motion and is observed in many side-chain LC polymers.^{14,16,17} Since the methylene spacer itself is nonpolar, its motion can be dielectrically active only if some adjacent polar group is connected to it, for example an oxygen atom.¹⁸ Generally, the spacer length does not strongly influence the parameters of γ relaxation, but in the side-chain LC polymer with a short spacer consisting only of two methylene groups, this dielectric transition is not observed.¹⁶ To make this motion possible, it is necessary to incorporate into the spacer a sequence of at least three methylene groups.¹⁹ In the present work we have used a spacer consisting of four methylene groups.

For the block copolymers under study the activation energy of the γ relaxation was $E_{a\gamma} = 30$ kJ/mol, and the relaxation time τ_γ lies in the interval $(2.3-1.5) \times 10^{-4}$ s (at -120 °C). The shape parameter α_{HN} has values in the range 0.25–0.27, which is typical for a secondary relaxation. It is clearly seen from Figure 5 that the confinement does not cause any variation in the γ relaxation parameters. On the basis of these results, we can conclude that the 1D-, 2D-, and 3D-confined LC blocks reveal nearly the same spacer motion as the bulk material. Remember, the smallest domain size is present in the PSLC 97/3 sample, where the LC block is 3D-confined into a sphere with a diameter of 9.4 nm (see Table 1).

β Relaxation. The dielectric β transition is determined by the rotation of the mesogenic side group about its long axis. This process has been detected in the glassy state for many side-chain LC polymers.^{14,16,20–22} At frequencies of 10^7 – 10^9 Hz it also should be active in the LC and the isotropic phases. A similar behavior is expected for the block copolymers investigated in the present work. In the mesomorphic state the β peak strongly overlaps with the more intensive γ regime. This gives rise to the additional difficulty of resolving them from the dielectric spectra. A good separation between both relaxations was only possible at temperatures below -50 °C (see Figure 2). The appearance of the dielectric β process in the LC block is related to the presence of a carbonyl group between the cyanobiphenyl mesogenic group and the spacer. The carbonyl group has a component of the dipole moment directed normal to the long axis of the mesogenic group. Although the nitrile group has a high dipole moment (4.2 D),²³ it does not provide any contribution to the dielectric β process because its dipole moment is directed coaxially to the long axis of the mesogenic group. As a whole, the relaxation time and the activation energy of a given motion are defined basically by the size of the mesogenic fragment and depend only slightly on the spacer length, except for the case of a short spacer consisting of two methylene groups, where an effective decoupling between the mesogen and the main-chain motions is not reached.^{21,22} When the spacer contains more than six methylene groups, the parameters of the β relaxation practically do not vary any more. In contrast to the “purely local” nature of the γ process, the β relaxation may be regarded to some extent as a cooperative one. Because of the relatively bulky phenyl rings involved in this, motion is influenced by strong steric interactions with the nearest environment. Taking into account this “dual” nature of the β transition, we may expect some effect under confinement on this motion. We also may expect that the origin of possible changes should be similar to those observed for the cooperative relaxation (dynamic glass transition or α process). Indeed, it follows from Figure 5 that the relaxation time as well as the activation energy for β transition decreases for a confined length less than 21 nm, whereas the shape parameter α_{HN} does not vary with experimental uncertainties. Interestingly, for the same copolymers we have found a speed-up of the cooperative dynamics (α and δ relaxation) at the same confined length.⁴ This fact suggests a common mechanism for cooperative and local β motions under spatial constraints. The overall change in relaxation time for the β process is about a half order of magnitude, which is considerably less than observed for essentially cooperative modes.

Let us turn to a cooperative aspect of the local modes. An alternative expression for eq 2 is given by Eyring's

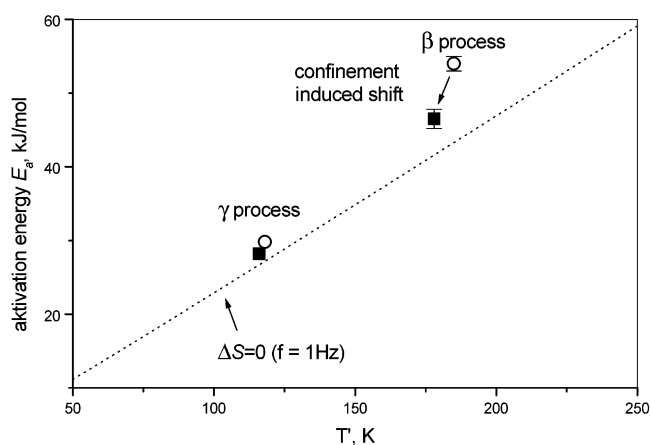


Figure 6. Activation energy E_a of local modes vs T for PSLC 0/100 (○) and PSLC 85/15 (■). The dotted line was calculated according to eq 3. T is the temperature at which the frequency of the relaxation is 1 Hz.

activated states equation:

$$f = 1/(2\pi\tau) = kT/(2\pi h) \exp(-\Delta H/RT) \exp(\Delta S/R) \quad (3)$$

where the R , k , and h are the gas constant, Boltzmann, and Planck constants, respectively. ΔH and ΔS are the activation enthalpy and entropy, respectively. We now calculate the activation energy E_a at frequency f' and the corresponding temperature T from the logarithmic derivative of τ with respect to $1/T$. This results in¹⁵

$$E_a = \Delta H + RT = RT[1 + \ln(kT/(2\pi hf'))] + T\Delta S \quad (4)$$

where f' and T are given in hertz and kelvin, respectively. For a noncooperative relaxation the activation entropy ΔS should be close to zero due to independent motion of kinetic units. On the basis of this idea, the relation between the activation energy E_a and the temperature T at which the frequency of the relaxation is 1 Hz is given by

$$E_a = RT[1 + \ln(k/2\pi h) + \ln T] = RT[22.92 + \ln T] \quad (5)$$

This relation does not contain any adjustable parameters and represents a universal line in coordinates E_a vs T . It has been shown that local relaxations agree well with the zero entropy prediction for a variety of polymers.¹⁵ For the essentially cooperative relaxations, such as the dynamic glass transition, it was proven that the data deviated significantly from the zero entropy prediction. Using this routine, we can now differentiate between noncooperative and cooperative motions. Figure 6 displays the activation energy E_a as a function of T for the β and γ relaxation in PSLC 0/100 and PSLC 85/15. In the latter the LC blocks are 2D-confined in cylinders with diameter of 12.6 nm. The dotted line was calculated according to eq 5. It is clearly seen from Figure 6 that the γ relaxation is close to the theoretical line, which defines an effective lower limit for the activation energies of noncooperative motions. The β process is considerably above the dotted line, proving the partial cooperative nature of that motion, i.e., that $\Delta S > 0$.¹⁵ The effect of confinement is visible as the shift of the β process in direction to the dotted line. This simply implies a reduction of cooperativity induced by confinement. In other words, the kinetic

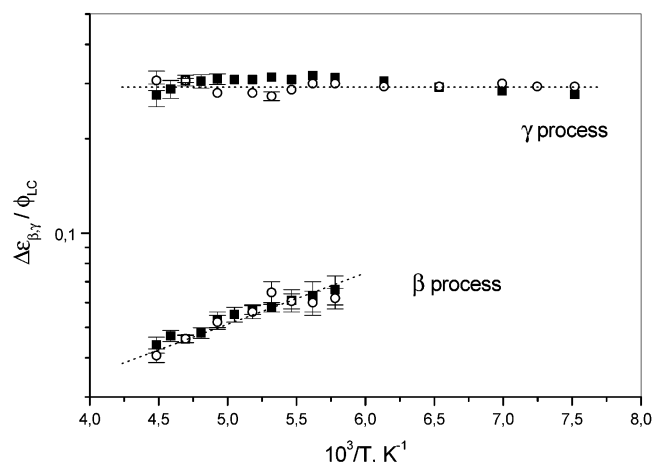


Figure 7. Relaxation strength $\Delta\epsilon$ normalized to the volume fraction of the LC block (ϕ_{LC}) vs reciprocal temperature for β and γ local modes in PSLC 0/100 (■) and PSLC 85/15 (○). The lines are a guide for the eyes.

units start to move more independently from each other in the confined state. This loss of cooperativity is also reflected in the temperature dependence of the relaxation rate. For cooperative motion the temperature dependence usually follows a Vogel–Fulcher–Tammann law. It is changed toward an Arrhenius-like law for the confined state.²⁵ The same effect may be analyzed with the fragility index m . Thin polymer films become less fragile as their thickness decreases.⁷ Secondary relaxations in polymers already have an Arrhenius-type temperature dependence of the relaxation rate, and we are able to detect only the small decreases of the activation energy and relaxation times in confined state. In general, this type of motion is determined by barrier heights of internal rotation and hence cannot strongly be influenced by confinement. Our results for the γ relaxation, which one can refer to as an “ideal local motion”, clearly demonstrate that.

The cooperative character of a relaxation process should also show in another feature of the dielectric relaxation. Figure 7 displays the relaxation strength $\Delta\epsilon$ normalized to the volume fraction of the LC block (ϕ_{LC}) vs reciprocal temperature for both local modes in PSLC 0/100 and PSLC 85/15. The $\Delta\epsilon_\beta$ and $\Delta\epsilon_\gamma$ values were obtained from fits of the isothermal dielectric loss data to the HN equation (eq 1). For an ideal local motion (no interaction between dipoles) the product $\Delta\epsilon T$ should be constant. It is clearly seen from Figure 7 that the γ relaxation in both compounds completely satisfies this condition; i.e., $\Delta\epsilon_\gamma \approx \text{constant}$ in coordinates $\Delta\epsilon - 1/T$ in a broad temperature range. At the same time, the $\Delta\epsilon_\beta$ increases with decrease of temperature, and therefore the effective dipole moment increases. This behavior is characteristic for cooperative type relaxations. These results confirm once more that the γ process may be considered as noncooperative, whereas the β is cooperative. It should be noted that from Figure 7 we do not see any confinement effect on both processes as the data from both selected samples fall on common lines. According to our previous consideration, this should be valid for γ relaxation but not for the β process. The origin for this lies in the higher uncertainty in $\Delta\epsilon/\phi_{LC}$ determination and the rather weak dependence of $\Delta\epsilon_\beta$ on confinement. In the case of segmental relaxation (α -process) in PMMA thin films the confinement effect on $\Delta\epsilon_\alpha$ is more pronounced.^{8,9} The $\Delta\epsilon_\alpha$ value decreases with decreasing film thickness, reflecting a loss of cooperativity. We point out that in the case of the β process

the values τ and E_a are more precisely determined and are sensitive to geometrical constraints (see Figure 6).

4. Conclusions

We have studied the local dynamics of PS/LC block copolymers, which reveal two local modes: γ and β , assigned to the LC block spacer motion and rotation of the mesogen fragment around its long axis, respectively. Because of a strong incompatibility between the PS block and the LC block, the copolymers are microphase-separated. As a result, the LC block is confined to domains with shape and size depending on the chemical composition. In the sample of smallest domain size the LC block is 3D-confined into a sphere with a diameter of 9.4 nm. The γ process is noncooperative and is not sensitive to spatial constraints, even for the smallest confined length. A surprising finding is that the β relaxation speeds up for confinement length less than ~ 20 nm. We suggest that its partially cooperative nature is responsible for this effect. In fact, the essentially cooperative modes (α and δ) of the LC block reveal the analogous behavior at the same confinement length.

Acknowledgment. We are grateful to the DFG (Grant STU 191-1) for financial support.

References and Notes

- (1) Goodman, I. *Developments in Block Copolymers*; Applied Science Publishers: London, 1982.
- (2) Floudas, G.; Paraskeva, S.; Hadjichristidis, N.; Fytas, G.; Chu, B.; Semenov, A. N. *J. Chem. Phys.* **1997**, *107*, 5502–5509.
- (3) Floudas, G.; Meramveliotaki, K.; Hadjichristidis, N. *Macromolecules* **1999**, *32*, 7496–7503.
- (4) Zhukov, S.; Geppert, S.; Stühn, B.; Staneva, R.; Ivanova, R.; Gronski, W. *Macromolecules* **2002**, *35*, 8521–8530.
- (5) Fukao, K.; Miyamoto, Y. *Europhys. Lett.* **1999**, *46*, 649–654.
- (6) Fukao, K.; Miyamoto, Y. *Phys. Rev. E* **2000**, *61*, 1743–1754.
- (7) Fukao, K.; Miyamoto, Y. *Phys. Rev. E* **2001**, *64*, 011803.
- (8) Fukao, K.; Uno, S.; Miyamoto, Y.; Hoshino, A.; Miyaji, H. *Phys. Rev. E* **2001**, *64*, 051807.
- (9) Hartmann, L.; Gorbatschow, W.; Hauwede, J.; Kremer, F. *Eur. Phys. J. E* **2002**, *8*, 145–154.
- (10) Wübbenhorst, M.; Murray, C. A.; Forrest, J. A.; Dutcher, J. R. *Proc. ISE-11*, Melbourne, Australia, 1–3 Oct 2002.
- (11) Zhukov, S.; Stühn, B.; Borisova, T.; Barmatov, E.; Barmatova, M.; Shibaev, V.; Kremer, F.; Pissis, P. *Macromolecules* **2001**, *34*, 3615–3625.
- (12) Zhong, Z.; Schuele, D.; Gordon, W. *Liq. Cryst.* **1994**, *17*, 199–209.
- (13) Havriliak, S.; Hegami, S. *J. Polym. Sci., Part C* **1966**, *14*, 99.
- (14) Gedde, U. W.; Liu, F.; Hult, A.; Sahlen, F.; Boyd, H. *Polymer* **1994**, *35*, 2056–2062.
- (15) Starkweather, Jr., H. W. *Macromolecules* **1988**, *21*, 1798–1802.
- (16) Zentel, R.; Strobl, G.; Ringsdorf, H. *Macromolecules* **1985**, *18*, 960–965.
- (17) Mosciicki, J. K. Dielectric relaxation in macromolecular liquid crystals. In *Liquid Crystal Polymers—From Structures to Applications*; Collyer, A. A., Ed.; Elsevier: Amsterdam, The Netherlands, 1992.
- (18) Wetton, R. E.; Williams, G. *Trans. Faraday Soc.* **1965**, *61*, 2132–2139.
- (19) Willbourn, A. H. *Trans. Faraday Soc.* **1958**, *54*, 717–729.
- (20) Schönhals, A.; Wolff, D.; Springer, J. *Macromolecules* **1995**, *28*, 6254–6257.
- (21) Schönfeld, A.; Kremer, F.; Hofmann, A.; Kühnpast, K.; Springer, J.; Scherowsky, G. *Makromol. Chem.* **1993**, *194*, 1149–1155.
- (22) Kremer, F.; Schönhals, A. *Broadband Dielectric Spectroscopy*; Springer-Verlag: Berlin, 2003; Chapter 10, pp 385–432.
- (23) Klinbiel, R. T.; Genova, D. J.; Criswell, T. R.; Meter, J. P. *J. Am. Chem. Soc.* **1974**, 7651.
- (24) Starkweather, Jr., H. W. *Polymer* **1991**, *32*, 2443–2448.
- (25) Kremer, F.; Huwe, A.; Arndt, M.; Behrens, P.; Schwieger, W. *J. Phys.: Condens. Matter* **1999**, *11*, A175–A188.